Article

Journal of the Brazilian Chemical Society

https://dx.doi.org/10.21577/0103-5053.20240184

*J. Braz. Chem. Soc.* **2025**, *36*, 4, e-20240184, 1-15


# Green and Effective: Chitosan Blends with Fish Collagen and *Aloe vera* Exudate

***Pâmella R. L. C. Gonçalves,[a] Rosiane S. Penha,[a] Jaciene J. F. Cardoso,[b] Amanda R. Guimarães[c] and Cícero Wellington B. Bezerra*** *[,d]

[a]*Rede de Biodiversidade e Biotecnologia da Amazônia Legal-Bionorte, Universidade Federal do Maranhão, 65080-805 São Luis-MA, Brazil*

[b]*Departamento de Tecnologia Química, Universidade Federal do Maranhão, 65080-805 São Luís-MA, Brazil*

[c]*Department of Organic Chemistry I, Centro de Innovación en Química Avanzada (ORFEO-CINQA), Universidad del País Vasco/Euskal Herriko Unibertsitatea (UPV/EHU) Po Manuel Lardizabal 3, E-20018 Donostia/San Sebastián, Spain*

[d]*Departamento de Química, Universidade Federal do Maranhão, 65080-805 São Luís-MA, Brazil*

Chitosan (CS) blends with collagen (CL) and *Aloe vera* (AV) have gained significant attention in the biomedical field due to their biocompatibility, biodegradability, and potential for wound healing applications. In this study, we investigated the preparation and characterization of CS/CL and CS/AV blends using selective precipitation and co-precipitation techniques. The synthesis processes were analyzed for yield and 4-hydroxyproline content (in CS/CL blends). The materials were characterized using bromatological analyses, viscosity measurements, Fourier-transform infrared spectroscopy (FTIR), X-ray diffraction (XRD), and scanning electron microscopy (SEM). These eco-friendly methods effectively promoted interactions between the biopolymers, resulting in homogeneous blends with tunable properties. Besides, they are simple, fast, safe, and require minimal infrastructure. This study demonstrated that selective precipitation and co-precipitation are effective methods for producing chitosan/collagen and chitosan/*Aloe vera* blends. These methods foster interactions and miscibility between the biopolymers, as confirmed by FTIR, XRD, viscosity, and 4-Hy content analyses. They also align with green chemistry principles by avoiding organic solvents, reducing environmental risks, and minimizing waste. The high yields achieved, especially for CS/AV blends (exceeding 96%), make these materials compatible with lyophilization procedures. The absence of segregated phases after appropriate washing underscores their suitability for pharmaceutical formulations and other applications.

**Keywords:** biomaterials, green syntheses, sustainable materials, natural polymers

## Introduction

Blends are homogeneous compounds formed by combining two or more different materials. Unlike simple mixtures, blends involve interactions between components, resulting in properties distinct from those of the individual materials. These properties can be synergistic, complementary, or intermediate, offering enhanced functionalities. Blends are crucial in materials science for their ability to combine the advantages of individual materials and develop new, improved properties.[1,2]

Chitosan (CS) is a linear polymer composed mainly of 2-amino-2-deoxy-D-glucose (glucosamine) units linked by β-(1-4) bonds. Derived from the deacetylation of chitin found in crustaceans, insects, and fungal cell walls, chitosan is valued for its biocompatibility, biodegradability, and antimicrobial properties. Its versatility makes it a popular starting material for creating polymer blends with other biopolymers to develop materials with functional properties.[3-5]

One commonly combined biopolymer with chitosan is hyaluronic acid (HA). CS/HA blends exhibit promising properties for tissue engineering, cartilage regeneration, dressings, and controlled drug release. The combination of antimicrobial and healing properties of chitosan with hydrophilic, bioadhesive, and biocompatible properties of HA results in materials suitable for these applications.[6,7]

Other biopolymers like gelatine, alginate, fibrin, carrageenan, and pectin have also been blended with

*e-mail: cwb.bezerra@ufma.br
Editor handled this article: Izaura C. N. Diógenes

chitosan. For instance, chitosan/gelatine blends offer controlled biodegradation and mechanical properties, making them suitable for tissue engineering, cell encapsulation, and contact lenses.[8-14] Chitosan/alginate blends, with their gelling properties and controlled drug release capacity, are used in drug delivery and tissue regeneration.[9,15]

Collagen (CL) is another biopolymer often blended with chitosan. Collagen, a primary component of the extracellular matrix in connective tissues, provides structural support and promotes cell adhesion. CS/CL blends have applications in tissue engineering, bone and skin regeneration, three-dimensional scaffolds, and advanced dressings. These blends benefit from biocompatibility of collagen and antimicrobial properties of chitosan, making them effective for preventing infections and promoting new tissue formation.[5,16-21]

CS/CL blends also hold potential in controlled drug release, allowing for prolonged and localized delivery of therapeutic substances. This is particularly relevant for treating chronic diseases where precise drug delivery is crucial.[22,23] Chitosan blends with *Aloe vera* (CS/AV) are another focus of research due to their combined properties. CS/AV blends are used to create bioactive dressings that effectively promote wound and ulcer healing. The moisturizing and anti-inflammatory properties of *Aloe vera*, combined with antimicrobial ability of chitosan, help prevent infection and accelerate skin regeneration.[24-29]

Various methods exist for preparing polymeric chitosan blends. Seidi *et al*.[30] and El-Hefian *et al*.[31] categorize the most common procedures into solution mixing and fusion mixing. Solution mixing, the most widely used due to its simplicity and versatility, involves dissolving the precursors in a suitable solvent and mixing them to form a homogeneous dispersion. The resulting solution undergoes treatment processes like solvent evaporation or freeze-drying to obtain a solid matrix of the biopolymer blends.[6,9,16,24,25] Melt blending involves combining chitosan and other polymers in a solid state and heating them to form a homogeneous molten mass.[32-34]

Other methods include enzyme immobilization, where enzymes act as cross-linking agents to enhance the stability, elasticity, and mechanical strength of the blends, and electrospinning, which creates nanofibers or thin films from biopolymer solutions.[35-41]

To reduce the environmental impacts of traditional synthesis methods, we have adopted sustainable principles of green chemistry. These principles focus primarily on waste reduction and the use of less toxic reagents. The aim is to minimize the adverse effects of chemical production through strategies such as the use of safer solvents and reagents, energy efficiency, and reduction of hazardous substances. Specifically, we employed a less hazardous synthesis approach, which involves using substances and methods that pose fewer risks to human health and the environment.[42]

Chitosan blends represent a promising area of research in biomaterials and tissue engineering. By combining the individual properties of biopolymers, these blends offer potential applications in regenerative medicine, controlled drug release therapy, food packaging, and wastewater treatment. Continued research and development of these blends could lead to improved clinical outcomes and patient quality of life.[43,44]

As many synthesis procedures do not distinguish well between the blends and the precursor biomaterials, this work developed routes of synthesis by selective precipitation and by co-precipitation for blends of chitosan with collagen and with the exudate of *Aloe vera*, respectively. In these procedures, the biopolymers are dissolved separately in aqueous solutions, and then the solutions are mixed gradually under constant stirring. Precipitation of the biopolymers (co-precipitation) occurs during mixing, resulting in the formation of solid or gelatinous particles containing the blend of *Aloe vera* and chitosan, for example, or precipitation can be promoted, in the case of collagen with chitosan, by the addition of salt or by pH control (selective precipitation). After precipitation, in both cases, the particles formed can be collected by centrifugation or filtration, followed by washing to remove impurities, and freeze-dried to obtain the final product in solid form. In different proportions, the CS/AV and CS/CG blends were characterized by Fourier-transform infrared spectroscopy (FTIR), X-ray diffraction (XRD), scanning electron microscopy, and viscometry. The individual characteristics of the biopolymer precursors, the interactions between them, and the effect of the chosen precipitating reagents were also investigated.

## Experimental

All chemicals used in this study were of analytical reagent grade. Acetic acid (99.7%, Isofar, Rio de Janeiro, Brazil), sulfuric acid (95%, Sigma-Aldrich, St. Louis, USA), hydrochloric acid PA (37%, Quimex, Minas Gerais, Brazil), ammonium hydroxide (28-30%, Isofar, Rio de Janeiro, Brazil), sodium hydroxide (97%, Quimex, Minas Gerais, Brazil), sodium chloride (99.5%, Isofar, Rio de Janeiro, Brazil), sodium hypochlorite (4-6%, Sigma-Aldrich, St. Louis, USA), silver nitrate (99.8%, Dinamica, Indaiatuba, São Paulo, Brazil), chloramine T (98%, Sigma-Aldrich, St. Louis, USA), *p*-dimethylaminobenzaldehyde

(> 99%, Sigma-Aldrich, St. Louis, USA), L-hydroxyproline (≤ 100%, Merck, São Paulo, Brazil) were used. All solutions were prepared using distilled water.

The chitosans (CS) used in this work are from two sources: commercial (degree of deacetylation (DD) = 75-85% = 449 kDa, Sigma-Aldrich, St. Louis, USA) and laboratory-prepared, obtained from the deacetylation of chitin extracted from the exoskeleton of white shrimp (*Litopenaeus vannamei*), purchased at the local fish market (São Luís, MA).[45] Both were purified before use by dissolving in acetic acid solution (0.5 mol $L^{-1}$) for 18 h, followed by filtration to eliminate insoluble entities, and precipitation with concentrated ammonium hydroxide. The CS samples were then washed with distilled water to neutrality and dried in an oven at 60 °C for 24 h.[46] The commercial CS was employed as reference material in the syntheses and, when not mentioned otherwise, the results presented will be those obtained from the laboratory-prepared CS. Both commercial and homemade chitosan were analyzed by titrimetric techniques to determine the degree of deacetylation (GD), showing values of 82 and 96%, respectively.

### Extraction of fish collagen

The fish collagen (CL) was extracted from the fresh swim bladder of the Gurijuba (*Hexanematichthys parkeri*) and Pescada Amarela (*Cynoscion acoupa*), acquired in the São Luís market (Maranhão-Brazil). The swim bladders were incised, washed thoroughly with distilled water, and immersed in acetic acid solution (pH 3.5) over 24 h (1.0 g of swim bladder *per* 20 mL of acetic acid). After being filtrated, the soluble collagen was salted out by addition of a NaCl saturated solution. Subsequently, the suspension was spun at 500 rpm, and washed with distilled water until complete removal of chloride ions (silver nitrate test). The obtained collagen (CL-HP, CL-CA) was dried and stored in a vacuum desiccator.[47]

### *Aloe vera* leaf exudate

Freshly harvested *Aloe vera* leaves (AV) were washed in tap water, sanitized in sodium hypochlorite solution (0.05%, under stirring and for 15 min) and then washed with distilled water. Next, the *Aloe vera* leaves were peeled to obtain the mucilaginous tissue. The internal gel was homogenized in a blender for 3 min at room temperature, filtered and frozen and changed in the form of lyophilized (at –70 °C, So-Low freezer, model U85-18, for 8 h; lyophilizer (Terroni, model Fauvel-LB1500, São Paulo, Brazil), –60 °C, for 48 h), and stored in a desiccator until further use.

### Preparation of CS/CL and CS/AV blends

#### CS/CL

Aqueous solutions of both polymers were prepared separately in 0.5 mol $L^{-1}$ acetic acid (pH = 2.5, 24 h) and then mixed (constant stirring, 24 h) in the following nominal precursor ratio CS:CL (m/m): 80:20; 50:50 and 20:80. CS/CL-HP and CS/CL-CA blends were separated from the aqueous medium by the following procedures: (*i*) freeze-drying (at –70 °C, So-Low freezer, model U85-18, for 8 h; Terroni lyophilizer, model Fauvel-LB1500, –60 °C, for 48 h); (*ii*) salt precipitation (NaCl 3 mol $L^{-1}$); (*iii*) alkaline precipitation ($NH_4OH_{(conc.)}$) and (*iv*) saline-alkaline precipitation (NaCl and $NH_4OH$). For cases (*ii*), (*iii*) and (*iv*), a white precipitate was observed, which was separated by centrifugation, washed with distilled water until the absence of base (pH control) and the chloride ions (addition of $AgNO_{3(aq)}$), followed by washing with acetone and drying in desiccator.

#### CS/AV

Since *Aloe vera* lyophilized was soluble in alkaline and acidic aqueous media, and did not precipitate by saline addition (NaCl), the synthesis procedure employed was coprecipitation by addition of $NH_4OH$ (precipitating agent for CS). In short, aqueous solutions of both biomaterials were prepared separately in 0.5 mol $L^{-1}$ acetic acid (pH = 2.5, 24 h) and then mixed in the following m/m CS:AV ratios 75:25; 50:50 and 25:75. During the $NH_4OH$ addition, there was the formation of a white precipitate that, similarly to the CS/CL blend, was separated by centrifugation, washed with distilled water to neutral pH and with acetone. The CS/AV blends were dried in an oven at 40 ºC for 12 h and placed in desiccator.

### Material characterization

#### 4-Hy (hydroxyproline) content

The quantification of collagen in the CS/CL blends was performed by determination of 4-Hy (hydroxyproline). In a typical experiment, 4 mL of 6 mol $L^{-1}$ hydrochloric acid was added to 1 mL of each soluble collagen sample (100 mg of collagen/blend for 100 mL of acetic acid). Hydrolysis was carried out at a temperature of 130 °C, for 24 h.[47] After that, the solution was neutralized by $NaOH_{(aq)}$ addition and the final volume was made up to 100 mL. To a 2 mL aliquot of this solution, 1 mL of 0.05 mol $L^{-1}$ chloramine T (prepared just before its use) was added and left at room temperature for 20 min for complete oxidation of hydroxyproline. Then, 1 mL of *p*-dimethyl-amino-benzaldehyde solution (15 g of *p*-dimethyl-amino-benzaldehyde, 60 mL of *n*-propanol,

26 mL of 70% perchloric acid were made up to a volume of 100 mL with distilled water) was added to develop the red-purple coloration, and the tubes were introduced into a water bath at 60 ºC for 15 min. Samples were left to cool to room temperature and the absorbance of the samples was recorded at a wavelength of 560 nm. The equipment used was a UV-Vis spectrophotometer (Varian, model Cary 50, Australia). Analytical curves were obtained for the following concentrations of 4-Hy: 0.5, 1.0, 2.0, 3.0 and 4.0 mg $L^{-1}$.

### Bromatological analyses

The bromatological assays of the lyophilized *Aloe vera* and pysceous collagen were performed according to the official methodologies indicated by the Adolfo Lutz Institute.[48] Humidity, ashes, lipids, proteins and carbohydrates were the analysis realized in this work.

### Viscosity measurements

The viscosity measurements were performed in a Cannon-Fenske Routine capillary viscometer (Herzog, model HVB-438) coupled to a thermostatic bath with temperature control (25 ± 0.5 °C). Assays were performed with solution of collagen, chitosan, *Aloe vera* and their respective blends at concentrations ranging from 2 to 6 g $L^{-1}$. The solvent used as calibration fluid was 0.5 mol $L^{-1}$ acetic acid, with a viscosity value ($\eta_0$) of 0.968 $mm^2$ $s^{-1}$. The flow times were recorded with an accuracy of ± 0.01 s, and all measurements were performed in triplicate and the average value was used. Before each measurement, the solutions were vacuum filtered.

The relative viscosities ($\eta_r$) were determined according to equation 1, were η, ν, and ρ are the dynamic viscosity, kinematic viscosity, and density of the polymer solution, respectively, and $\eta_0$, $\nu_0$, $\rho_0$, the corresponding values for the solvent. As the solution densities did not differ significantly from that of the solvent, $\eta_r$ could be estimated from the ratio of the efflux time of the polymeric solution and the solvent. From the values of the relative viscosities, the specific viscosities, $\eta_{sp}$, were determined in accordance with equation 2. The values of the specific viscosities, in turn, were employed for the definition of the reduced viscosities ($\eta_{red}$) (equation 3, where *c* is the concentration of the polymeric solution, in g $mL^{-1}$), which, by graphic method ($\eta_{red} \times c$, extrapolation of the straight line obtained by linear regression) the values of the intrinsic viscosities were established [η] (equation 4).[49]

$$\eta_r = \frac{\eta}{\eta_0} = \frac{\rho\nu}{\rho_0\upsilon_0} \approx \frac{t}{t_0} \quad (1)$$

$$\eta_{sp} = \eta_r - 1 \quad (2)$$

$$\eta_{red} = \frac{\eta_{sp}}{c} \quad (3)$$

$$[\eta] = \lim_{c \to 0} \eta_{red} \quad (4)$$

The viscosity-average molecular weight (MW) of the chitosan and collagen were obtained from the intrinsic viscosity values using the Mark-Houwink equation (equation 5), where κ and α are constants that depend on the interactions of polymer and solvent at a given temperature:[50,51]

$$[\eta] = \kappa(MW)^{\alpha} \quad (5)$$

### Fourier transform infrared spectroscopy

Fourier transform infrared spectroscopy (FTIR) analyses were carried out to inspect any interaction between the chitosan and the functional groups of the others biopolymers. Infrared spectra were recorded by a FT-IR Spectrometer (Shimadzu model IRPrestige-21, Kyoto, Japan) at room temperature, in the range between 4000 and 400 $cm^{-1}$, after grinding the materials and dispersing then in KBr matrix.

### X-ray diffraction (XRD)

The phases and crystalline structure present in the material were determined using X-ray diffraction, XRD (PANalytical, X'Pert PRO MPD PW 3040/60, Netherlands). The XRD measurements were performed with Theta/theta geometry and a Pixel 1D detector, utilizing monochromatic Kα radiation (λ = 1.540598 Å) form a cooper tube. Data were recorded under specific conditions: voltage set to 45 kV and current at 40 mA. The scans were collected over an angular range 0-70º (2θ) with measurements taken at intervals of 0.0131º (2θ) and a counting time of 7.564 s *per* data point.

### Scanning electron microscopy

Biopolymers and biopolymers blend micrographs were obtained using a scanning electron microscope, SEM (Phenom Pro X, Eindhoven, Netherlands), operating with primary electrons of 20 keV, with carbon films as support. For this analysis, the solid-state samples were deposited on a piece of carbon tape and placed in the sample holder, three regions being chosen in each composition.

## Results and Discussion

### Blends preparation

Yield calculations of CS:CL blend preparations are not

usually extensively investigated. Probably this is because freeze-drying and solvent evaporation techniques are widely employed methods. In our case, the yields merely indicate the ease of precipitation depending on the precipitating agent used. The results are presented in Figure 1.

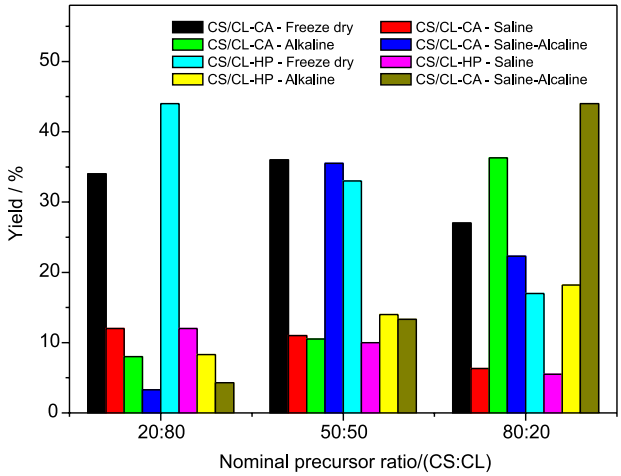


**Figure 1.** Synthesis yields (%) of chitosan/collagen blends (CS/CL) based on nominal precursor ratios. CA (*Cynoscion acoupa*, Pescada Amarela) and HP (*Hexanematichthys parkeri*, Gurijuba).

Previous works[47,52] have well-established that chitosan is pH-responsive in aqueous media. It forms soluble and viscous solutions at low pH values and becomes insoluble at high pH values. The hypothesis was that the addition of NaOH would facilitate chitosan precipitation, resulting in higher yields for blends with a higher chitosan content, whereas the addition of salt would favor blends with a higher nominal collagen participation.[53] Similarly, the results of saline-alkaline precipitations were expected to surpass the previous precipitations and approach the values obtained through the lyophilization process.

The results did not exactly follow these expected trends, but some generalizations can be interred. The freeze-drying procedure did not result in the highest yields in all cases. This can be justified by the fact that this technique removes water from the materials more efficiently compared to conventional drying performed on the precipitates obtained. Considering that water is an intrinsic component of collagen, the loss by sublimation during freeze-drying may be responsible for the lower yields observed.[54] Furthermore, it is noteworthy that some blends with the highest nominal percentage of collagen (20:80) exhibited the lowest values for precipitation methods.

Another important aspect is that the lowest yields were observed for the saline precipitation route. In fact, depending on the NaCl added, collagen exhibits the salting-in effect (at low concentrations) and the salting-out effect (at higher concentrations).[55] Thus, by manipulating the NaCl concentration, collagen can be selectively precipitated based on its molecular weight, but such precipitation is not always quantitative. Lin *et al.*[56] extracted collagens from the skin of bigeye tuna (*Thunnus obesus*) using two different methods, isoelectric precipitation and salting-out, and found that the lowest yield (14.14%) was observed through saline precipitation. Sadowska *et al.*[53] investigated the precipitation of collagen using sodium chloride and k-carrageenan, an acid polysaccharide especially rich in sulfate groups. Their study revealed that the yield of collagen precipitation from its solution depended on the solvent used for collagen extraction, pH, ionic strength and precipitating agent concentration. The authors did not observe any collagen precipitation in alkaline environments even with k-carrageenan.

The precipitation behavior of CS/CL-CA and CS/CL-HP blends exhibited a clear correlation with the specific precipitation medium. In alkaline conditions, primarily favoring chitosan precipitation, yield increased proportionally with chitosan content, as evidenced by the CS/CL-CA (8, 10.5, and 36.5%) and CS/CL-HP (8.3, 14, and 18.2%) blends, respectively. Conversely, saline media, which preferentially induce collagen precipitation, resulted in higher yields for blends with greater nominal collagen content: 12, 11, and 6.3% for CS/CL-CA and 12, 10, and 5.5% for CS/CL-HP (20:80, 50:50, and 80:20 ratios). These findings underscore the selective precipitation induced by the specific medium, highlighting the influence of blend composition and precipitating agents on yield.

The 4-hydroxyproline (4-Hy) content of collagens extracted from the swim bladders of Pescada Amarela (*Cynoscion acoupa*) and Gurijuba (*Hexanematichthys parkeri*) fish were 34.0 and 47.6 mg $g^{-1}$, respectively. This corresponds to estimated collagen contents of 272 and 382.4 mg *per* gram of swim bladder. As shown in Table 1,

**Table 1.** Bromatological composition of samples of *Aloe vera* freeze-dried (AV) and collagens (CL) from the swim bladders of Gurijuba (HP, *Hexanematichthys parkeri*) and Pescada Amarela (CA, *Cynoscion acoupa*)

| Sample | Ash / % | Humidity / % | Lipid / % | Crude fiber / % | Protein / % | Carbohydrate / % |
|---|---|---|---|---|---|---|
| AV | 18.81 ± 1.24 | 11.68 ± 1.77 | 6.12 ± 0.18 | 0.059 ± 0.03 | 2.75 ± 0.66 | 60.58 ± 0.78 |
| CL-HP | 0.67 ± 0.14 | 13.2 ± 0.24 | – | – | 89.98 ± 0.98 | – |
| CL-CA | 0.57 ± 0.11 | 14.56 ± 0.49 | – | – | 88.91 ± 0.68 | – |

Mean ± standard deviation (n = 3).

swim bladders consist mainly of protein, accounting for approximately 89% of their dry weight.

The content of 4-Hy is dependent on various factors, including the species, age, tissue, habitat, body temperature of the animals, as well as the collagen extraction process itself, which can lead to fragmentation and losses.[57] Therefore, these values need to be considered with caution. Varied contents of 4-Hy for different tissues can be found in the literature. For instance, Uriarte-Montoya *et al.*[58] reported a content of 6.5% in squid mantles (skins); Ramasamy and Sahanmugam,[59] found 7.55 in mollusk mantles (Sepia), Prestes *et al.*[60] observed 3.53 in bovine collagen, and Gauza-Włodarczyk *et al.*,[61] reported a content of 5.68% for salmon of the species *Salmo salar* L.

The content of 4-Hy is an important marker because this particular amino acid is exclusively found in collagen and elastin. Therefore, it can be presumed that the entire 4-Hy content detected in the samples is attributed to the presence of collagen. In fact, the amount of 4-Hy can be used as an estimate of the collagen content in a sample by considering the proportion in which it occurs in the collagen structure. In this case, the proportion is 12.5 g of 4-Hy *per* 100 g of collagen,[62-64] which corresponds to a conversion factor equal to 8.

Based on these 4-Hy values and assuming a constant conversion factor, the nominal ratios of chitosan blends CS/CL-CA and CS/CL-HP (80:20, 50:50, and 20:80) would theoretically allow for maximum collagen contents in the blends of 54.4, 136, and 217 mg $g^{-1}$, and 76.6, 191, and 305.6 mg $g^{-1}$, respectively.

The results of the analysis on 4-Hy in the CS/CL blends are presented in Figure 2. Two important considerations arise from these findings. The first is that collagen is present in all precipitation methods employed, suggesting a spontaneous interaction with chitosan. The second observation is that no stoichiometric relationship was observed between the nominal collagen composition used in the synthesis and the actual amount detected. This lack of stoichiometry could indicate a saturation point in the effective interactions, which might not have been reached under certain precipitation conditions due to the presence of preferred interaction pathways that arise from each specific set of precipitation conditions.

Considering the importance of collagen content in the blends to ensure better performance in biomedical applications, owing to its biocompatible and regenerative properties, along with the advantages of alkaline precipitation in obtaining these materials, despite not being the highest yielding option, the CS/CL-HP 50:50 blend was chosen for subsequent studies.

Another aspect that influenced the selection of alkaline precipitation as the preparation method for CS/CL blends was its successful application in obtaining CS/AV blends, allowing for direct comparisons. Exudate solutions of AV did not exhibit the salt out effect under the employed conditions, and alkaline co-precipitation was the only viable technique in addition to freeze-drying. In fact, solubility experiments showed that 0.101 g of AV could dissolve in 30 mL of 0.5 mol $L^{-1}$ acetic acid solution (pH = 2.5). After complete dissolution, the solution was filtered, resulting in a retained mass of 0.003 g on the filter. Sodium hydroxide was added to the filtered solution, and no precipitate was observed, only a reversible change in color from colorless to yellow. Similarly, *Aloe vera* exudate was found to be soluble in water and did not precipitate upon addition of NaCl until the concentration of this salt reached 3 mol $L^{-1}$.

Despite the high solubility of *Aloe vera* exudate in aqueous media (acidic and alkaline), the yields obtained in the production of CS/AV blends in the ratios 75:25, 50:50, and 25:75 were remarkable, as shown in Figure 3. There was a positive variation with respect to the CS proportion in

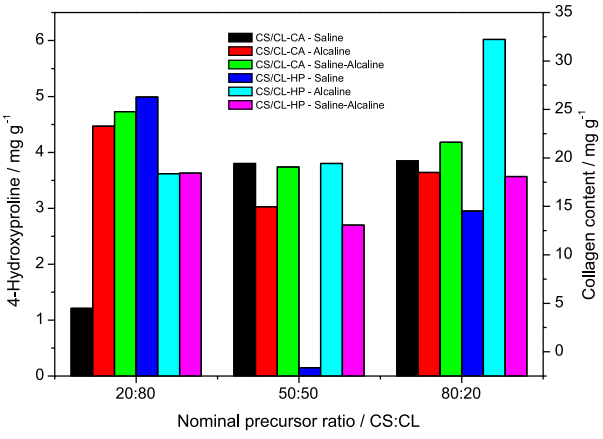


**Figure 2.** Content of 4-hydroxyproline (4-Hy) and collagen in CS/CL blends.

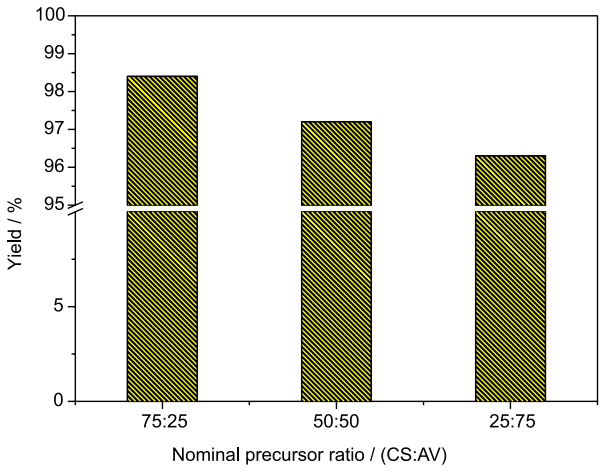


**Figure 3.** Synthesis yields (%) of chitosan/*Aloe vera* blends (CS/AV) based on nominal precursor ratios.

the blend, even for lower quantities of chitosan (25% of the nominal mass), where the amount of precipitated material exceeded 96% of the nominal mass, indicating excellent co-precipitation of *Aloe vera*. Such significant difference in yield between the chitosan blends with *Aloe vera* (AV) and those with collagen (CL) can be attributed to the distinct composition of these biopolymers (as shown in Table 1) and their interactions with chitosan. Specifically, components like glucomannan, mannan, and acemannan in *Aloe vera* are known to enhance compatibility and interaction with chitosan.[65-67] Studies by Bajer *et al*.[68] and Khoshgozaran-Abras *et al*.[69] support this notion, demonstrating strong interactions between *Aloe vera* and chitosan in blended films, leading to decreased water solubility and reduced water vapor permeability with increasing *Aloe vera* content.

### Bromatological composition of collagen and *Aloe vera*

The results of the bromatological analyses are presented in Table 1. These assays provide important information regarding the composition and quality of the materials, which is essential for their characterization and evaluation in various applications, particularly in biomedical contexts. Excessive moisture, for example, can compromise the stability and durability of the materials, as well as affect their physical and chemical properties. The presence of inorganic substances is relevant, especially in blends intended for biomedical applications, as it indicates the potential presence of undesired components in biological environments. Knowledge of the lipid content is crucial as it impacts solubility, stability, drug release, and interactions with biological systems. Proteins play essential roles in biological processes and can influence the biocompatibility, cellular adhesion, and drug release capacities of the materials. Carbohydrate analysis is significant for understanding the physical properties, biodegradability, and interactions with biological systems of the materials.

As expected, the composition reveals the diverse nature of these two classes of biopolymers, collagen and *Aloe vera*, which implies their distinct applications. The collagen materials demonstrate a proteinaceous nature, while *Aloe vera* stands out for its high concentration of carbohydrates. Both characterizations are consistent with findings in the literature, except for the fiber content (AV), which yielded a percentage value of 0.059 ± 0.03% due to the filtration method proposed in this study, below the reported literature value of 12.31 ± 2.18%.[59,60,70-73]

### Viscosity and viscosity-average molecular weight

The viscometry characterization was used to determine the molecular weight of the employed chitosan and collagen, as well as to verify changes in the viscosity of the medium due to blend formation. Although it is not an absolute method, viscometry is a frequently used technique for figuring out the molecular weight of polymers.

Using κ and α values according to Kasaai *et al*.,[51] in the Mark-Houwink equation (equation 5), the commercial CS exhibited intrinsic viscosity [η] and viscosity-average molecular weight (MW) values of 725.3 and $3.7 \times 10^5$ g mol$^{-1}$, respectively. Such MW value is in the same order of magnitude as that indicated by the manufacturer ($4.5 \times 10^5$ g mol$^{-1}$), hence supporting the experimental setup and adopted methodology. The laboratory-prepared CS exhibited a [η] of 358.8 mL g$^{-1}$ and MW of $7.07 \times 10^4$ g mol$^{-1}$, which is also consistent with literature reports for chitosan in the range of $10^4$ to $10^6$ g mol$^{-1}$.[74]

The collagen isolated from the swim bladder of the Gurijuba fish (CL-HP) had a [η] of 182.52 mL g$^{-1}$ and MW of $9.0 \times 10^7$ g mol$^{-1}$, taking κ and α values of $1.66 \times 10^{-8}$ L g$^{-1}$ and 0.885, respectively.[75] Few studies are available regarding the determination of collagen viscosity-average molecular weight, making comparisons difficult. However, when denatured collagen was used in Porto's work,[76] the predicted MW was $1.8 \times 10^7$ g mol$^{-1}$, which is comparable with the result that was provided.

*Aloe vera* exudate is a complex material comprising carbohydrates, organic acids, salts, enzymes, saponins, polyphenols, among other components.[77] Since this is a mixture there is no reason, therefore, to establish the MW. Under the employed conditions, AV exhibited an intrinsic viscosity of 189.2 mL g$^{-1}$, similar to that of CL-HP.

The changes in reduced viscosity of biopolymer solutions due to the mixing at the established ratios are shown in Figures 4a-4b. Notably, the blends exhibit intermediate reduced viscosity values compared to those of the isolated biopolymers. Furthermore, a positive trend of increasing viscosity is observed with increasing chitosan content in the blend. These findings are consistent with those reported by Ye *et al*.,[78] in a study on the miscibility of collagen/chitosan blends in dilute solutions, where they reported higher viscosity for chitosan compared to collagen solutions, as well intermediate values for the viscosity for the produced blends at different biopolymers compositions. The authors concluded that intermolecular interactions are responsible for the miscibility of both polymers, regardless of concentration or aggregation state.

Interestingly, the CS/AV blend exhibits a significantly higher viscosity compared to the CS/CL blend, even at a lower chitosan concentration (50% *vs*. 20%). This suggests that the interaction between CS and AV is more specific and substantial compared to the interaction with

CL. It is even plausible that, in addition to the expected intermolecular interactions, AV components can interact directly with chitosan chains, establishing a highly cross-linked structure that positively impacts the viscosity of the solution. In fact, cationic chitosan can interact with specific proteins and polysaccharides of *Aloe vera*, potentially through ionic interactions or hydrogen bonding, leading to stronger interactions than those with protein groups present in collagen.[25,65,68,79,80] Consequently, it is plausible that AV molecules not only participate in intermolecular interactions but also interact with chitosan chains to form a highly cross-linked structure, resulting in a high viscosity solution. This crosslinking effect reinforces the intermolecular interactions, collectively explaining the high viscosity values observed for CS/AV mixture solutions compared to CS/CL mixtures.

On the other hand, the increasing viscosity sequence observed in chitosan-collagen blends, with chitosan exhibiting the highest viscosity, does not necessarily indicate miscibility loss. This trend may be related to the enhanced favorable interactions between protonated chitosan (in acetic acid medium) with the solvent, intensifying intermolecular forces and raising solution viscosity. Several studies[78,81] have demonstrated that chitosan and collagen are miscible at molecular scale in solution in various solvents at room temperature, even in different proportions.

## Fourier transform infrared spectroscopy

Figures 5 and 6 depict the infrared (FTIR) vibrational spectra of the biopolymers and one of their corresponding blends. Table 2 summarizes the main assignments given to the all spectra.

Chitosan (commercial and laboratory-prepared CS indicated in parenthesis, $cm^{-1}$) exhibited characteristic vibrational bands. The range of 3800-3000 $cm^{-1}$ (3680-2990) was attributed to the ν(OH), ν(NH) vibrations. The peaks at 2927 and 2876 $cm^{-1}$ (2938 and 2883, respectively) corresponded to symmetric and asymmetric ν(CH), originating from $–CH_2$ and $–CH_3$ groups. The band at 1662 $cm^{-1}$ (1655) was attributed to ν(C=O) stretching of the residual N-acetyl groups (amide I band). At 1593 $cm^{-1}$ (1573) there was a δ(N–H) bending of the primary amine. A peak at 1414 $cm^{-1}$ (1408) was assigned to stretching vibrations of ν(OH) from the primary alcoholic group.[16] The band at 1379 $cm^{-1}$ (1336) was attributed to stretching of amide III, ν(C–N). Finally, the range of 1162-845 $cm^{-1}$ was characteristic of the polysaccharide structure for both types of chitosan. The presented attributions are consistent with the current literature.[16,43,82]

In the collagen (CL-HP, Figure 5c) vibrational spectrum, the prominent bands were detected at a range of 3700-3000 $cm^{-1}$ attributed to the ν(OH), ν(NH) stretching vibrations; 2927 and 2866 $cm^{-1}$ (weak) corresponding to symmetric and asymmetric $\nu(CH)_s$ and $\nu(CH)_{as}$, respectively; 1662 $cm^{-1}$ relative to the amide I band; 1555 $cm^{-1}$ (amide II), attributed to δ(N–H) bending and ν(CN) vibrations in plane; 1459 $cm^{-1}$ corresponding to the vibrations of pyrrolidine rings in proline and hydroxyproline; 1345 $cm^{-1}$ $\nu(CH)_{as}$, attributed to in-plane vibrations of amide III, involving ν(CN) stretching and δ(N–H) deformation.[56]

In Figure 6c, the vibrational spectrum of lyophilized AV is presented. The following vibrational transition were observed: a range of 3690-3000 $cm^{-1}$, attributed to the ν(OH) and ν(NH) stretching characteristic of amino acids; peaks at 2945 and 2897 $cm^{-1}$ due to symmetrical and asymmetrical stretching of C–H present in the $–CH_2$ group, as well as aliphatic –CH groups present in the compounds. The peak at 1628 $cm^{-1}$ was assigned to the amide I band, indicating the presence of carbonyl groups, ν(C=O). The

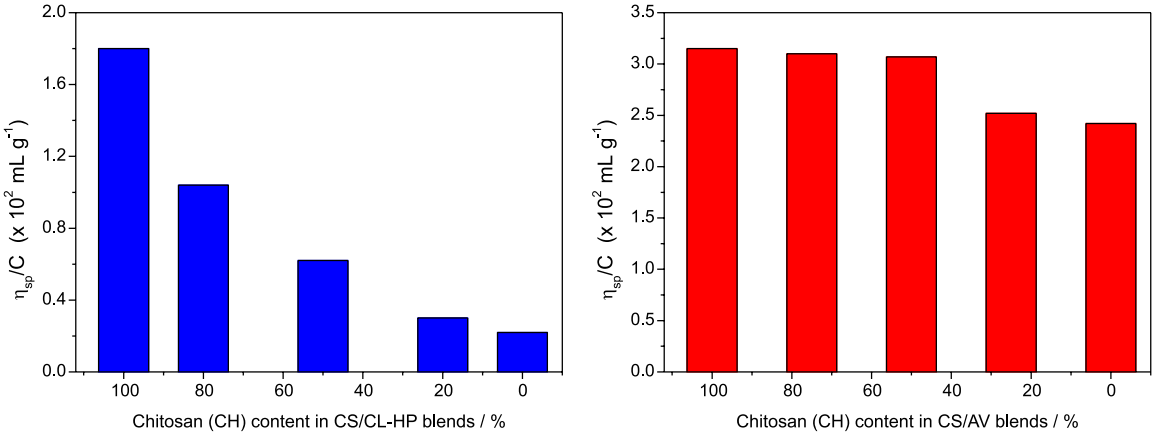


**Figure 4.** Reduced viscosity values of the biopolymers isolated and their blends (total concentration ($C_T$) = 4 mg $L^{-1}$): (a) CS/CL-HP; (b) CS/AV, against CS percentage.

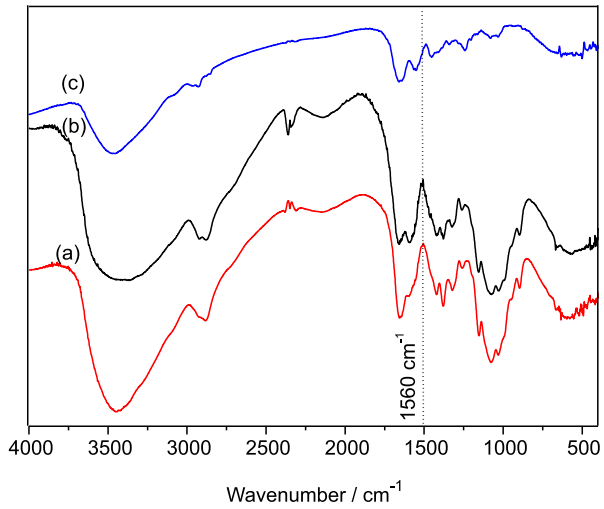


**Figure 5.** FTIR (KBr) spectra of chitosan (CS) (a), collagen (CL) (c) and their corresponding 50:50 blend (CS/CL-50:50) (b).

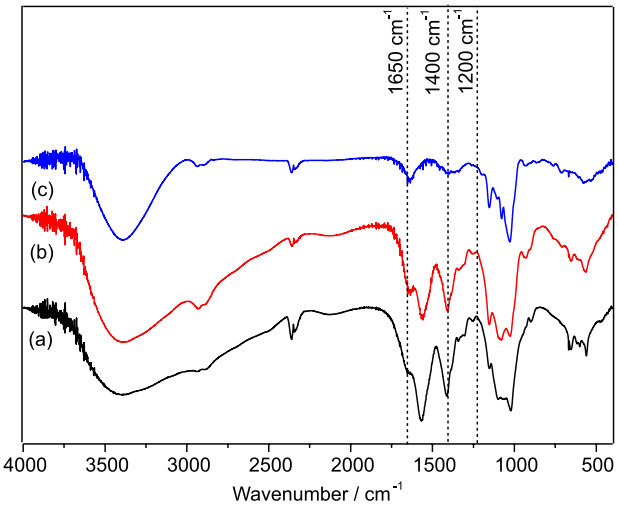


**Figure 6.** FTIR (KBr) spectra of chitosan (CS) (a), *Aloe vera* (AV) (c) and their corresponding blend (CS/AV-50:50) (b).

broad band centered around 1408 $cm^{-1}$ was attributed to the presence of carboxylic components.[83] A peak at 1139 $cm^{-1}$ was assigned to the stretching vibrations of C=S bond, and a peak at 856 $cm^{-1}$ was attributed to the vibrations of CH in the pyranose ring.[83,84]

In general, it can be observed that the vibrational profiles of isolated biopolymers are quite similar, making it difficult to draw a conclusive statement about the interactions and blend formation using only this technique. However, in the products formed by precipitation (CS/CL) and co-precipitation (CS/AV), characteristic vibrational transitions of both biopolymers can be distinguished, along with alterations in some vibrational bands, confirming the presence of both in the blends. This is consistent with the results of the 4-Hy analysis, which indicated the presence of collagens in the CS/CL blends, the spectra exhibited a broader band in the OH and NH vibration region, related to the proteinaceous material. Additionally, there were higher intensities of the peak at ca. 1560 $cm^{-1}$, attributed to a greater number of NH groups.[58,85]

Similarly, in the CS/AV blends, predominant vibrational transitions characteristics of the chitosan were observed. However, as observed by Zarandona *et al.*,[24] and Jithendra *et al.*,[84] the spectra revealed distinct elements compared to pure chitosan, suggesting interactions with components of *Aloe vera* through slight shifts and alteration in the shape of certain bands. As depicted in Figure 6, the blend exhibits sharper peaks at ca. 1650 $cm^{-1}$ ν(C=O),

**Table 2.** Main vibrational transitions and their respective assignments for the biopolymers (CS, CL, AV) and their blends

| Wavenumber / $cm^{-1}$ | | | | | | | | | | Assignment |
|---|---|---|---|---|---|---|---|---|---|---|
| CS[a] | CL | CS:CL 80:20 | CS:CL 50:50 | CS:CL 20:80 | CSb | AV | CS:AV 75:25 | CS:AV 50:50 | CS:AV 25:75 | |
| 37000-2990 | 3700-3000 | 3800-2990 | 3800-2900 | 3800-2990 | 3685-2990 | 3690-3000 | 3685-2997 | 3700-2990 | 3680<br>2997 | ν(OH)<br>ν(NH) |
| $2927_w$ | $2927_w$ | 2922 | 2922 | 2922 | 2938 | 2945 | 2927 | 2935 | 2927 | $\nu(CH)_s$ |
| 2876 | 2855 | 2871 | 2871 | 2881 | 2883 | 2897 | 2876 | 2894 | 2869 | $\nu(CH)_a$ |
| 1655 | 1662 | 1657 | 1657 | 1657 | 1655 | 1628 | $1634_{sh}$ | 1652 | 1644 | ν(C=O) |
| 1596 | 1555 | 1596 | 1585 | 1596 | 1573 | – | 1575 | 1565 | 1593 | ν(–NH) |
| 1420 | 1459 | 1429 | 1429 | 1426 | 1408 | 1408 | – | 1414 | 1420 | ν(OH)<br>$\nu(COO–)_s$ |
| 1383 | 1345 | 1374 | 1374 | 1374 | 1336 | 1353 | 1373 | 1341 | 1379 | ν(–CN) |
| 1159 | – | 1161 | 1159 | 1161 | 1159 | 1156 | 1152 | 1153 | 1152 | $\nu(C–N)_{ring}$ |
| 1080 | 1079 | 1076 | 1076 | 1076 | 1015 | 1080 | 1084 | 1088 | 1079 | ν(CO) |
| 1029 | 1039 | 1029 | 1029 | 1029 | – | 1031 | 1026 | 1021 | 1031 | ν(C=S) |
| 891 | – | 888 | 898 | 898 | 897 | 856 | 895 | – | 891 | $\nu(C–H)_{ring}$ |

[a]Commercial CS; [b]laboratory-prepared CS. w and sh represent weak and shoulder, respectively.

ca. 1400 $cm^{-1}$ ν($COO^-$), and ca. 1200 $cm^{-1}$ ν(C=S) due to presence of AV components.

While conclusive evidence is lacking, the spontaneous co-precipitation of *Aloe vera* and collagen with chitosan, combined with observed variations in viscosity and subtle infrared spectroscopic signatures consistent with published reports, suggest that hydrogen bonding, electrostatic interactions, and van der Waals forces are the primary drivers for interactions between these biopolymers. Specifically, chitosan and collagen (CS/CL) likely interact primarily through hydrogen bonding between the amino groups of chitosan and the carbonyl groups within peptide bonds of collagen. However, these interactions appear weaker and less extensive compared to those observed in CS/AV blends. This difference translates to lower viscosimetric properties and potentially limited miscibility between CS and CL. In contrast, chitosan seems to interact with anionic polysaccharides of *Aloe vera* through strong electrostatic interactions. Additionally, hydrogen bonds form between the hydroxyl groups in chitosan and the carboxyl and hydroxyl groups present in *Aloe vera* components. These more extensive interactions likely explain the higher viscosity and potentially better miscibility observed in CS/AV blends compared to CS/CL blends.[86,87]

## X-ray diffraction

The crystallographic structures of the starting materials-commercial chitosan, laboratory-prepared chitosan, *Aloe vera*, and collagen-were investigated using XRD and presented in Figures 7 and 8. Commercial chitosan exhibited a characteristic semicrystalline profile, with prominent peaks at 2θ around 10º and 23º corresponding to the 020 and 110 crystal planes, respectively, consistent with previous reports.[24] These peaks indicate the presence of ordered crystalline regions within the chitosan structure.

*Aloe vera*, on the other hand, displayed a more crystalline pattern, marked by intense peaks at 2θ = 29.5º and 31.7º, which corroborate previous findings.[88] The XRD patterns of the chitosan/*Aloe vera* blends (CS/AV) demonstrated distinct profiles from both precursor biopolymers, suggesting structural modifications resulting from their interaction. However, the blends resembled the diffraction profile of chitosan more closely than that of *Aloe vera* exsudate, aligning with our FTIR data. This observation suggests that the chitosan structure plays a more dominant role in the blended materials. Further analysis of the blend diffractograms revealed small shifts in peak positions, a decrease in intensity, and peak broadening. These observations indicate interactions between chitosan and *Aloe vera* exudate components, reflecting the compatibility of the biopolymers and potential structural integration within the matrix.[68,80] These interactions likely contribute to the altered molecular arrangement observed in the blends, supporting the hypothesis of enhanced amorphous characteristics.

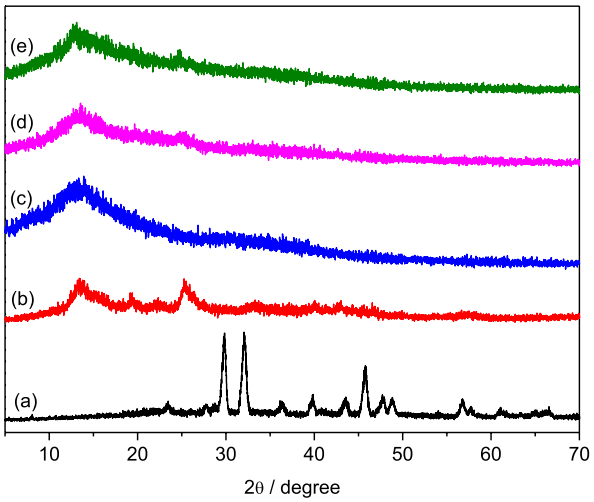


**Figure 7.** XRD spectra of (a) *Aloe vera*; (b) chitosan laboratory-prepared (CS); (c) CS/AV-25:75; (d) CS/AV-50:50 and (e) CS/AV-75:25.

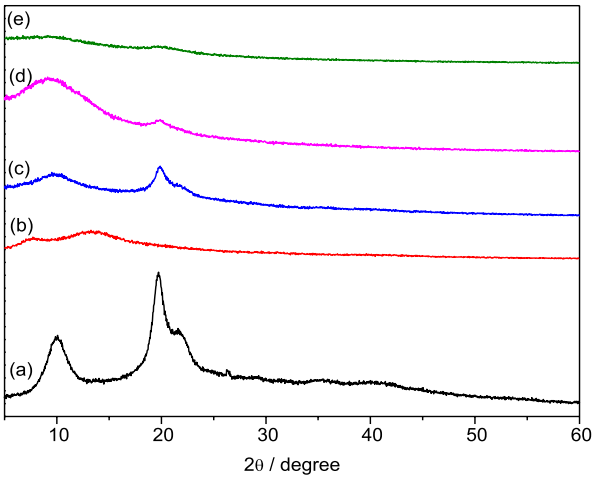


**Figure 8.** XRD spectra of (a) chitosan comercial (CS), (b) collagen (CL), (c) CS/CL-80:20, (d) CS/CL-50:50 and (e) CS/CL-20:80.

Collagen, as expected, exhibited greater amorphous features, as evidenced by the absence of well-defined peaks in its XRD pattern. The blends displayed intermediate characteristics between the two precursors, corroborating our viscosity and infrared analysis results. Interestingly, as the chitosan content increased in the blends, the corresponding reflections in the XRD patterns became more pronounced. This observation suggests that the compatibility between the biopolymers and their interactions are significantly influenced by the chitosan concentration. Higher chitosan content likely promotes stronger intermolecular interactions, leading to a more ordered structure and enhanced crystallinity.[13,80,87,89]

## Morphological analysis

All samples were analyzed using SEM to examine the topography, roughness, miscibility, and distribution of materials in the blends. Figures 9 and 10 display images for chitosan (CS) and *Aloe vera* (AV) and their derivatives, with magnifications of 600× and 1200×, respectively. Figures 11 and 12 present the images for collagen (CL) and its derivatives at 400× and 1000× magnification, respectively.

Notably, Figures 9a and 9b highlight significant morphological differences between the precursors, CS and AV. Chitosan exhibits a granular and more amorphous appearance, while freeze-dried *Aloe vera* shows a fibrous and spongy structure. The SEM images of the CS/AV blends, as depicted in Figures 9 and 10, reveal intermediate profiles between these precursors. These blends exhibit smoother and more homogeneous surfaces, suggesting excellent miscibility between the biopolymers, consistent with the characterization data presented earlier. Yoshida *et al*.[25] reported that AV extract disperses well in chitosan without phase separation after blend drying, further supporting our findings. The variation in nominal composition also affects the morphological characteristics of the CS/AV blends. As the *Aloe vera* content increases, the uniformity of the matrix improves, indicating enhanced dispersion and interaction between the biopolymers.[86]

In contrast, the SEM images of the collagen blends (Figures 11 and 12) reveal a rougher, more irregular, and

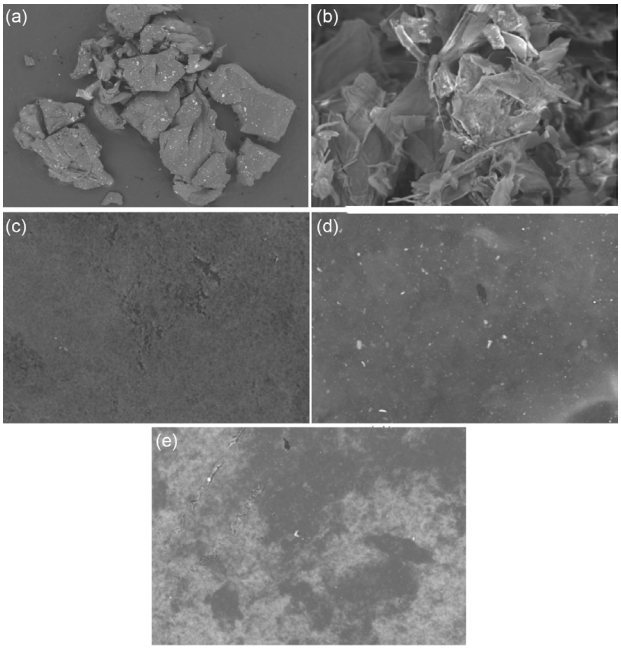


**Figure 9.** Scanning microscopy images of (a) chitosan (CS); (b) *Aloe vera* (AV) and CS/AV blends (alkaline precipitation): (c) 75:25; (d) 50:50; (e) 25:75. Magnification: 600×.

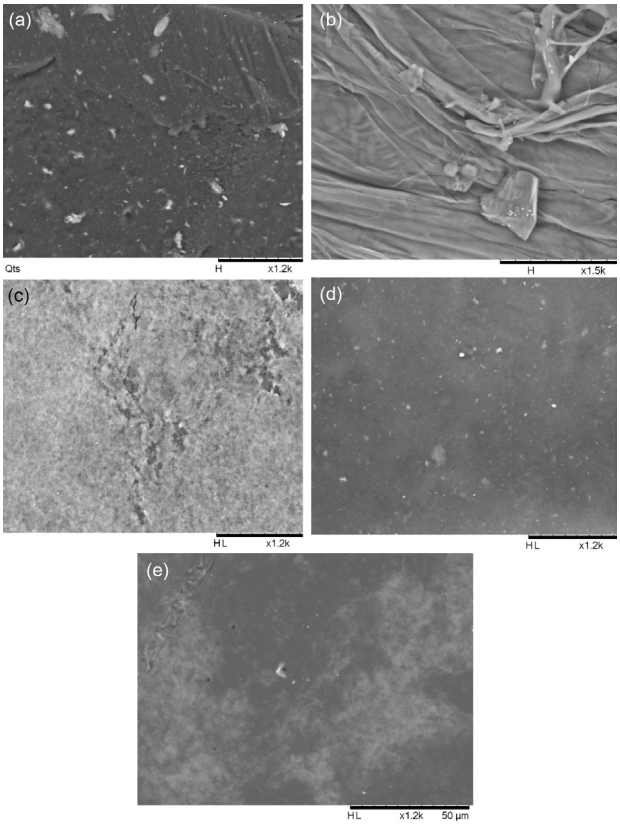


**Figure 10.** Scanning microscopy images of (a) chitosan (CS); (b) *Aloe vera* (AV) and CS/AV blends (alkaline precipitation): (c) 75:25; (d) 50:50; (e) 25:75. Magnification: 1200×.

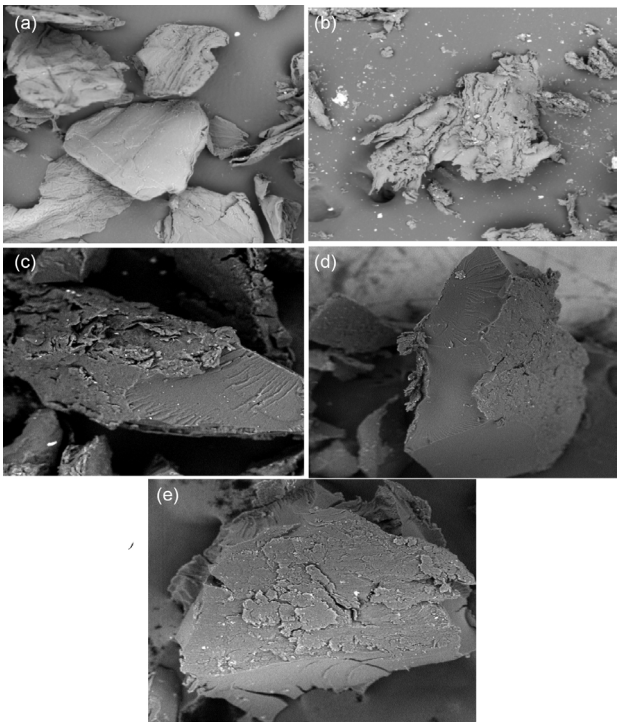


**Figure 11.** Scanning microscopy images of (a) chitosan (CS); (b) Collagen-HP (CL), and CS/CL blends (alkaline precipitation): (c) 80:20; (d) 50:50; (e) 20:80. Magnification: 400×.

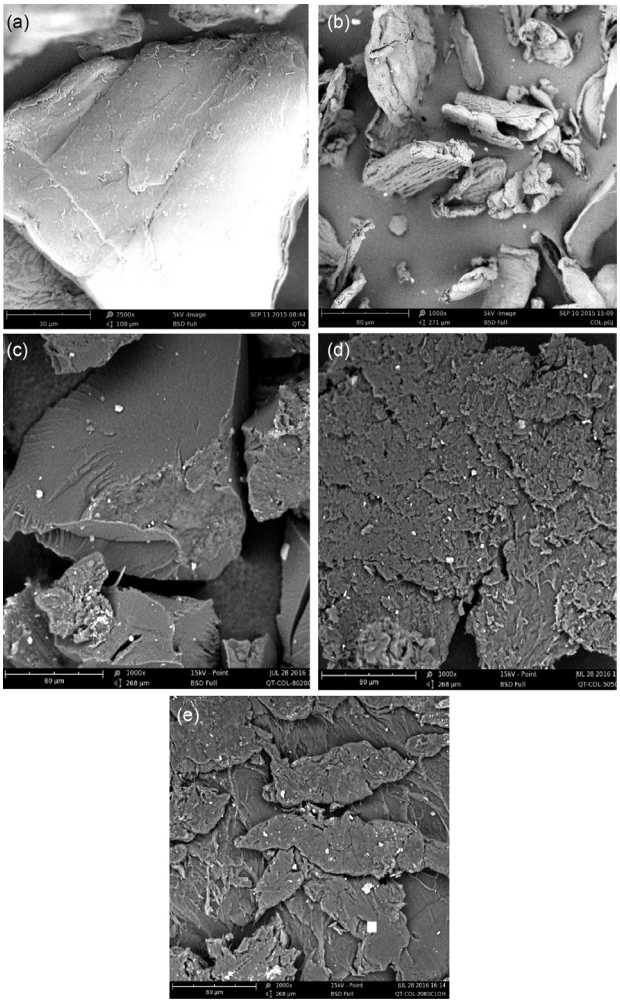


**Figure 12.** Scanning microscopy images of (a) chitosan (CS); (b) Collagen-HP (CL) and CS/CL blends (alkaline precipitation): (c) 80:20; (d) 50:50; (e) 20:80. Magnification: 1000×.

heterogeneous material formation compared to the CS/AV blends. Despite this, the collagen blends exhibit greater uniformity than pure collagen, demonstrating intermediate topography and roughness between their precursor materials. This observation suggests that both components, CS and CL, are well integrated into the blend, contributing to a more balanced morphological profile.

Overall, the SEM analysis demonstrates that the CS/AV blends exhibit superior miscibility and more homogeneous morphologies compared to the CS/CL blends. The morphological differences observed between the two types of blends can be attributed to the distinct interactions between the biopolymers, as indicated by the viscosity, FTIR, and XRD results. These findings highlight the compatibility and interaction dynamics of the biopolymer blends, providing valuable insights into their structural properties.

Notably, Figures 9a and 9b highlights significant differences in the morphologies of the precursors (CS and AV). While chitosan appeared in a granular and more amorphous form, freeze-dried *Aloe vera* exhibited a fibrous and spongy arrangement. The CS/AV blends Figures 9a and 9b, as expected and consistent with the characterization data presented earlier, showed intermediate profiles between the precursors, with smoother and more homogeneous surfaces, indicating excellent miscibility between the biopolymers.

By observing the collagen blends (Figures 11 and 12), it is evident that they displayed a rougher, more irregular, and heterogeneous material formation compared to the CS/AV blends. However, among the collagen blends themselves, they appeared to be more uniform than pure collagen, displaying intermediate topography and roughness between their precursor materials. These finding suggest the presence of both components (CS and CL) in the obtained materials.

## Conclusions

The present study successfully demonstrates the feasibility and efficiency of selective precipitation and co-precipitation methods for producing chitosan-based blends incorporating collagen and *Aloe vera*. These methods do not require sophisticated equipment, making them accessible for a wide range of applications. Besides, they showed high yields obtained, especially for the chitosan/*Aloe vera* blends, which exceeded 96%. Comprehensive characterization, including FTIR, XRD, viscosity measurements, and 4-Hy content analysis, confirmed the formation of homogeneous and stable blends with robust interactions between components.

A significant advantage of these routes is the avoidance of organic solvents, which aligns with the principles of green chemistry by reducing environmental risks and minimizing waste. This eco-friendly approach is further enhanced by the high yields obtained, especially for the chitosan/*Aloe vera* blends, which exceeded 96%. Such efficiency makes these methods highly compatible with lyophilization procedures, ensuring that the final products retain desirable properties for subsequent applications.

The enhanced viscosity observed in chitosan/*Aloe vera* blends suggests stronger intermolecular interactions compared to chitosan/collagen blends. This finding, coupled with the XRD data, supports the hypothesis of a more extensive cross-linked network within the chitosan/ *Aloe vera* matrix. These unique properties render the developed blends promising candidates for pharmaceutical applications demanding homogeneity and stability.

## Acknowledgments

The authors are grateful to FAPEMA and the European Commission (MSCA-IF-101026616) for the financial support and PRLCG thanks CAPES for the scholarship granted.

### Author Contributions

Cícero W. B. Bezerra was responsible for conceptualization, data curation, formal analysis, funding acquisition, investigation, methodology, project administration, resources, software, supervision, validation, visualization, writing original draft, review and editing; Pâmella R. L. C. Gonçalves for conceptualization, data curation, formal analysis, funding acquisition, investigation, methodology, project administration, resources, software, supervision, validation, visualization, writing original draft, review and editing; Rosiane S. Penha for conceptualization, formal analysis, funding acquisition, investigation, methodology, project administration, resources, software, supervision, validation, visualization, writing original draft; Jaciene J. Cardoso for conceptualization, formal analysis, investigation, methodology, validation, writing original draft; Amanda R. Guimarães for conceptualization, data curation, formal analysis, investigation, methodology, supervision, validation, visualization, writing original draft.

## References

1. Work, W. J.; Horie, K.; Hess, M.; Stepto, R. F. T.; *Pure Appl. Chem*. **2004**, *76*, 1985. [Crossref]
2. Ye, B.; Wu, B.; Su, Y.; Sun, T.; Guo, X.; *Polymers* **2022**, *14*, 4566. [Crossref]
3. Zhang, R.; Chang, S. J.; Jing, Y.; Wang, L. Y.; Chen, C.-J.; Liu, J.-T.; *Carbohydr. Polym.* **2023**, *314*, 120890. [Crossref]
4. Jayakumar, A.; Menona, D.; Manzoor, K.; Nair, S. V.; *Carbohydr. Polym.* **2010**, *82*, 227. [Crossref]
5. Ressler, A.; Ohlsbom, R.; Žužić, A.; Gebraad A.; Frankberg, E. J.; Pakarinen, T.-K.; Ivanković, H.; Miettinen, S.; Ivanković, M.; *Eur. Polym. J*. **2023**, *194*, 112129. [Crossref]
6. Phunpee, S.; Ruktanonchai, U. R.; Chirachanchai, S.; *Biomacromolecules* **2022**, *23*, 5361. [Crossref]
7. Valachová, K.; Šoltés, L.; *Molecules* **2021**, *23*, 1195. [Crossref]
8. Peter, M.; Ganesh, N.; Selvamurugan, N.; Nair, S. V.; *Carbohydr. Polym.* **2010**, *80*, 414. [Crossref]
9. Lawrie, G.; Keen, I.; Drew, B.; Chandler-Temple, A.; Rintoul, L.; Fredericks, P.; Grøndahl, L.; *Biomacromolecules* **2007**, *8*, 2533. [Crossref]
10. Ducret, M.; Montembault, A.; Josse, J.; Pasdeloup, M.; Celle, A.; Benchrih, R.; Mallein-Gerin, F.; Alliot-Licht, B.; David, L.; Farges, J. C.; *Dent Mater*. **2019**, *35*, 523. [Crossref]
11. Qureshi, M. A. R.; Arshad, N.; Rasool, A.; Islam, A.; Rizwan, M.; Haseeb, M.; Rasheed, T.; Bilal, M.; *Starch* **2022**, *76*, 2200052. [Crossref]
12. Martău, G. A.; Mihai, M.; Vodnar, D. C.; *Polymers* **2019**, *11*, 1837. [Crossref]
13. Yadav, R. P.; Chauhan, M. K.; *Int. J. Pharm. Sci. Res.* **2017**, *2*, 6. [Link] accessed in August 2024
14. Ravi Kumar, M. N. V.; *React. Funct. Polym.* **2000**, *46*, 1. [Crossref]
15. Baysal, K.; Aroguz, A. Z.; Adiguzel, Z.; Baysal, B. M.; *Int. J. Biol. Macromol.* **2013**, *59*, 342. [Crossref]
16. Sionkowska, A.; Wisniewski, M.; Skopinska, J.; Kennedy, C. J.; Wess, T. J.; *Biomaterials* **2004**, *25*, 795. [Crossref]
17. Ferreira, A. C.; Bomfim, M. R. Q.; da Costa Sobrinho, C. H. B.; Boaz, D. T. L.; Lira, R. S.; Fontes, V. C.; Arruda, M. O.; Zago, P. M. W.; Filho, C. A. A. D.; Dias, C. J. M.; Borges, M. O. R.; Ribeiro, R. M.; Bezerra, C. W. B.; Penha, R. S.; *AMB Express* **2022**, *12*, 102. [Crossref]
18. Thongchai, K.; Chuysinuan, P.; Thanyacharoen, T.; Techasakul, S.; Ummartyotin, S.; *SN Appl. Sci.* **2020**, *2*, 255. [Crossref]
19. Filipowska, J.; Lewandowska-Łańcucka, J.; Gilarska, A.; Niedźwiedzki, L.; Nowakowska, M.; *Int. J. Biol. Macromol.* **2018**, *113*, 692. [Crossref]
20. Deng, C.; Zhang, P.; Vulesevic, B.; Kuraitis, D.; Li, F.; Yang, A. F.; Griffith, M.; Ruel, M.; Suuronen, E. J.; *Tissue Eng., Part A* **2010**, *16*, 3099. [Crossref]
21. Yan, L.-P.; Wang, Y. J.; Ren, L.; Wu, G.; Caridade, S. G.; Fan, J. B.; Wang, L. Y.; Ji, P. H.; Oliveira, J. M.; Oliveira, J. T.; Mano, J. F.; Reis, R. L.; *J. Biomed. Mater. Res. A* **2010**, *95*, 465. [Crossref]
22. Hongsa, N.; Thinbanmai, T.; Luesakul, U.; Sansanaphongpricha, K.; Muangsin, N.; *Carbohydr. Polym.* **2022**, *277*, 118858. [Crossref]
23. Sachdeva, B.; Sachdeva, P.; Negi, A.; Ghosh, S.; Han, S.; Dewanjee, S.; Jha, S. K.; Bhaskar, R.; Sinha, J. K.; Paiva-Santos, A. C.; Jha, N. K; Kesari, K. K.; *Mar. Drugs* **2023**, *21*, 211. [Crossref]
24. Zarandona, I.; Minh, N. C.; Trung, T. S.; Caba, K.; Guerrero, P.; *Int. J. Biol. Macromol.* **2021**, *182*, 1331. [Crossref]
25. Yoshida, C. M. P.; Pacheco, M. S.; Moraes, M. A.; Lopes, P. S.; Severino, P.; Souto, E. B.; Silva, C. F.; *Polymers* **2021**, *13*, 1187. [Crossref]
26. Añibarro-Ortega, M.; Pinela, J.; Barros, L.; Ćirić, A.; Silva, S. P.; Coelho, E.; Mocan, A.; Calhelha, R. C.; Soković, M.; Coimbra, M. A.; Ferreira, I. C. F. R.; *Antioxidants* **2019**, *8*, 444. [Crossref]
27. de Oliveira Filho, J. G.; Lira, M. M.; de Sousa, T. L.; Campos, S. B.; Lemes, A. C.; Egea, M. B.; *Food Hydrocolloids Health* **2021**, *1*, 100012. [Crossref]
28. Ranjbar, R.; Yousefi, A.; *Bull. Emerg. Trauma* **2018**, *6*, 8. [PubMed]
29. Chabala, L. F. G.; Cuartas, C. E. E.; López, M. E. L.; *Mar. Drugs* **2017**, *15*, 328. [Crossref]

30. Seidi, F.; Yazdi, M. K.; Jouyandeh, M.; Dominic, M.; Naeim, H.; Nezhad, M. N.; Bagheri, B.; Habibzadeh, S.; Zarrintaj, P.; Saeb, M. R.; Mozafari, M.; *Int. J. Biol. Macromol*. **2021**, *183*, 1818. [Crossref]
31. El-Hefian, E. A.; Nasef, M. M.; Yahaya, A. H.; *J. Chem. Soc. Pak.* **2014**, *36*, 11. [Link] accessed in August 2024
32. Correlo, V. M.; Boesel, L. F.; Bhattacharya, M.; Mano, J. F.; Neves, N. M.; Reis, R. L.; *J. Mater. Sci. Eng. A* **2005**, *403*, 57. [Crossref]
33. Ghaderi, J.; Hosseini, S. F.; Keyvani, N.; Gómez-Guillén, M. C.; *Food Hydrocolloids* **2019**, *95*, 122. [Crossref]
34. Janik, W.; Wojtala, A.; Pietruszka, A.; Dudek, G.; Sabura, E.; *Polymers* **2021**, *13*, 2685. [Crossref]
35. Gajšek, M.; Jančič, U.; Vasić, K.; Knez, Ž.; Leitgeb, M.; *J. Cleaner Prod.* **2019**, *240*, 118218. [Crossref]
36. Chen, T.; Embree, H. D.; Brown, E. M.; Taylor, M. M.; Payne, G. F.; *Biomaterials* **2003**, *24*, 2831. [Crossref]
37. Savoca, M. P.; Tonoli, E.; Atobatele, A. G.; Verderio, E. A. M.; *Micromachines* **2018**, *9*, 562. [Crossref]
38. Badali, E.; Hosseini, M.; Mohajer, M.; Hassanzadeh, S.; Saghati, S.; Hilborn, J.; Khanmohammadi, M.; *Polym. Sci., Ser. A* **2021**, *63*, 1. [Crossref]
39. Law, J. X.; Liau, L. L.; Saim, A.; Yang, Y.; Idrus, R.; *Tissue Eng. Regener. Med*. **2017**, *14*, 699. [Crossref]
40. Pakravan, M.; Heuzey, M.-C.; Ajji, A.; *Biomacromolecules* **2012**, *13*, 412. [Crossref]
41. de Cassan, D.; Becker, A.; Glasmacher, B.; Roger, Y.; Hoffmann, A.; Gengenbach, T. R.; Easton, C. D.; Hänsch, R.; Menzel, H.; *J. Appl. Polym. Sci.* **2020**, *137*, 48650. [Crossref]
42. Jiang, A.; Li, J.; J. Shah, K.; You, Z. In *Green Chemistry for Environmental Sustainability - Prevention-Assurance-Sustainability (P-A-S) Approach*; Shah, K., ed.; IntechOpen, 2023. [Crossref]
43. dos Santos, C. C.; Mouta, R.; Castro Junior, M. C.; Santana, S. A. A.; Silva, H. A. D. S.; Bezerra, C. W. B.; *Carbohydr. Polym.* **2018**, *180*, 182. [Crossref]
44. Flórez, M.; Rodríguez, E. G.; Cazón, P.; Vázquez, M.; *Food Hydrocolloids* **2022**, *124*, 107328. [Crossref]
45. Zelencova, L.; Erdogan, L. S.; Baran, T.; Kaya, M.; *Polym. Sci., Ser. A* **2015**, *57*, 437. [Crossref]
46. dos Santos, J. E.; Soares, J. P.; Dockal, E. R.; Campana Filho, S. P.; Cavalheiro, É. T. G.; *Polímeros* **2003**, *13*, 242. [Crossref]
47. Fernandes, R. M.; Couto Neto, R. G.; Paschoal, C. W.; Rohling, J. H.; Bezerra, C. W. B.; *Colloids Surf., B* **2008**, *62*, 17. [Crossref]
48. Zenebon, O.; Pascuet, N. P.; Tiglea, P.; *Métodos Físico-Químicos para Análise de Alimentos*, 4th ed.; Instituto Adolfo Lutz: São Paulo, 2008.
49. Alsarra, I. A.; Betigeri, S. S.; Zhang, H.; Evans, B. A.; Neau, S. H.; *Biomaterials* **2002**, *23*, 3637. [Crossref]
50. Rinaudo, M.; *Prog. Polym. Sci.* **2006**, *31*, 603. [Crossref]
51. Kasaai, M. R.; Arul, J.; Charlet, G.; *J. Polym. Sci., Part B: Polym. Phys.* **2000**, *38*, 2591. [Crossref]
52. Xu, H.; Matysiak, S.; *Chem. Commun*. **2017**, *53*, 7373. [Crossref]
53. Sadowska, M.; Kołodziejska, I.; *Food Chem.* **2005**, *91*, 45. [Crossref]
54. Masic, A.; Bertinetti, L.; Schuetz, R.; Chang, S.-W.; Metzger, T. H.; Buehler, M. J.; Fratzl, P.; *Nat. Commun*. **2015**, *6*, 5942. [Crossref]
55. Duan, L.; Li, J.; Li, C.; Li, G.; *Korea-Australia Rheology J.* **2013**, *25*, 137. [Crossref]
56. Lin, X.; Chen, Y.; Jin, H.; Zhao, Q.; Liu, C.; Li, R.; Yu, F.; Chen, Y.; Huang, F.; Yang, Z.; *Mar. Drugs* **2019**, *17*, 261. [Crossref]
57. Nurilmala, M.; Suryamarevita, H.; Hizbullah, H. H.; Jacoeb, O. Y.; *Saudi J. Biol. Sci.* **2022**, *29*, 1100. [Crossref]
58. Uriarte-Montoya, M. H.; Arias-Moscoso, J. L.; Plascencia-Jatomea, M.; Santacruz-Ortega, H.; Rouzaud-Sández, O.; Cardenas-Lopez, J. L.; Marquez-Rios, E.; Ezquerra-Brauer, J. M.; *Bioresour. Technol.* **2010**, *101*, 4212. [Crossref]
59. Ramasamy, P.; Shanmugam, A.; *Int. J. Biol. Macromol.* **2015**, *74*, 93. [Crossref]
60. Prestes, R. C.; Golunski, S. M.; Toniazzo, G.; Kempka, A. P.; Luccion, M.; *Revista Brasileira de Produtos Agroindustriais* **2013**, *15*, 375. [Link] accessed in September 2024
61. Gauza-Włodarczyk, M.; Kubisz, L.; Włodarczyk, D.; *Int. J. Biol. Macromol.* **2017**, *104*, 987. [Crossref]
62. Sotelo, C. G.; Comesaña, M. B.; Ariza, P. R.; Pérez-Martín, R. I.; *J. Aquat. Food Prod. Technol.* **2015**, *25*, 388. [Crossref]
63. Amirrah, I. N.; Lokanathan, Y.; Zulkiflee, I.; Wee, M. F. M. R.; Motta, A.; Fauzi, M. B.; *Biomedicines* **2022**, *10*, 2307. [Crossref]
64. Blanco, M.; Vázquez, J. A.; Pérez-Martín, R. I. G.; Sotelo, C.; *Mar. Drugs* **2019**, *17*, 40. [Crossref]
65. Iqbal, D. N.; Munir, A.; Abbas, M.; Nazir, A.; Ali, Z.; Alshawwa, S. Z.; Iqbal, M.; Ahmad, N.; *Dose Response* **2023**, *21*, 15593258231169387. [Crossref]
66. Warkoyo; Purnomo, I.; Siskawardani, D.; Husna, A.; *Food Res.* **2022**, *6*, 298. [Crossref]
67. Silva, S. S.; Popa, E. G.; Gomes, M. E.; Cerqueira, M.; Marques, A. P.; Caridade, S. G.; Teixeira, P.; Sousa, C.; Mano, J. F.; Reis, R. L.; *Acta Biomater.* **2013**, *9*, 6790. [Crossref]
68. Bajer, D.; Janczak, K.; Bajer, K.; *J. Polym. Environ.* **2020**, *28*, 1021. [Crossref]
69. Khoshgozaran-Abras, S.; Azizi, M. H.; Hamidy, Z.; Bagheripoor-Fallah, N.; *Carbohydr. Polym.* **2012**, *87*, 2058. [Crossref]
70. Kittiphattanabawon, P.; Benjakul, S.; Visessanguan, W.; Shahidi, F.; *LWT - Food Sci. Technol.* **2010**, *43*, 792. [Crossref]
71. Singha, D.; Jubayer, M. F.; Devnath, K.; Akhter, D.; Ranganathan, T. V.; Rahman, M. T.; Mazumder, M. A. R.; *J*. **2021**, *4*, 430. [Crossref]

72. Farid, A.; Tawfik, A.; Elsioufy, B.; Safwat, G.; *Int. J. Parasitol.: Drugs Drug Resist*. **2021**, *17*, 156. [Crossref]
73. Muñoz, O. M.; Leal, X.; Quitral, V.; Cardemil, L.; *Med. Aromat. Plants* **2015**, *4*, 3. [Crossref]
74. Kubota, N.; Eguchi, Y.; *Polym. J*. **1997**, *29*, 123. [Crossref]
75. Voron'ko, N. G.; Derkach, S. R.; Vovk, M. A.; Tolstoy, P. M.; *Carbohydr. Polym.* **2016**, *151*, 1152. [Crossref]
76. Porto, L. C.: *Filmes Formados por Gelatina e Poli (Acrilamida-co-Ácido Acrílico): Efeito da Composição, do Plastificante e Agente Reticulante nas Propriedades Térmicas, Mecânicas e Absorção de Água*; MSc Dissertation, Federal University of Santa Catarina, Florianópolis, 2007. [Link] accessed in August 2024
77. Nejatzadeh-Barandozi, F.; *Org. Med. Chem. Lett.* **2013**, *3*, 5. [Crossref]
78. Ye, Y.; Dan, W.; Zeng, R.; Lin, H.; Dan, N.; Guan, L.; Mi, Z.; *Eur. Polym. J.* **2007**, *43*, 2066. [Crossref]
79. Lewandowska, K.; Sionkowska, A.; Grabska, S.; *J. Mol. Liq*. **2015**, *212*, 879. [Crossref]
80. Kumar, H. M. P. N.; Prabhakar, M. N.; Prasad, C. V.; Rao, K. M.; Reddy, T. V. A. K.; Rao, K. C.; Subha, M. C. S.; *Carbohydr. Polym.* **2010**, *82*, 251. [Crossref]
81. Wei, W.; Zhou, Y.-H.; Chang, H.-J.; Yeh, J.-T.; *J. Macromol. Sci., Part B* **2015**, *54*, 143. [Crossref]
82. Queiroz, F. M.; Melo, K. R.; Sabry, D. A.; Sassaki, G. L.; Rocha, H. A.; *Mar. Drugs* **2014**, *13*, 141. [Crossref]
83. Fardsadegh, B.; Jafarizadeh-Malmiri, H.; *Green Process. Synth.* **2019**, *8*, 399. [Crossref]
84. Jithendra, P.; Rajam, A. M.; Kalaivani, T.; Mandal, A. B.; Rose, C.; *ACS Appl. Mater. Interfaces* **2013**, *5*, 7291. [Crossref]
85. Pereda, M.; Ponce, A. G.; Marcovich, N. E.; Ruseckaite, R. A.; Martucci, J. F.; *Food Hydrocolloids* **2011**, *25*, 1372. [Crossref]
86. Devernois, E.; Coradin, T.; *Gels* **2023**, *9*, 518. [Crossref]
87. Felicia, W. X. L.; Rovina, K.; Mamat, H.; Aziz, A. H. A.; Lim, L. S.; Jaziri, A. A.; Nurdiani, R.; *Appl. Food Res.* **2024**, *4*, 100439. [Crossref]
88. Prabhakar, S.; OjhaNupur, D. N.; *Water Sci. Technol.* **2020**, *82*, 2446. [Crossref]
89. Chen, Z.; Mo, X. He, C.; Wang, H.; *Carbohydr. Polym.* **2008**, *72*, 410. [Crossref]

*Submitted: July 27, 2024*
*Published online: September 16, 2024*